Suppl. Fig 1

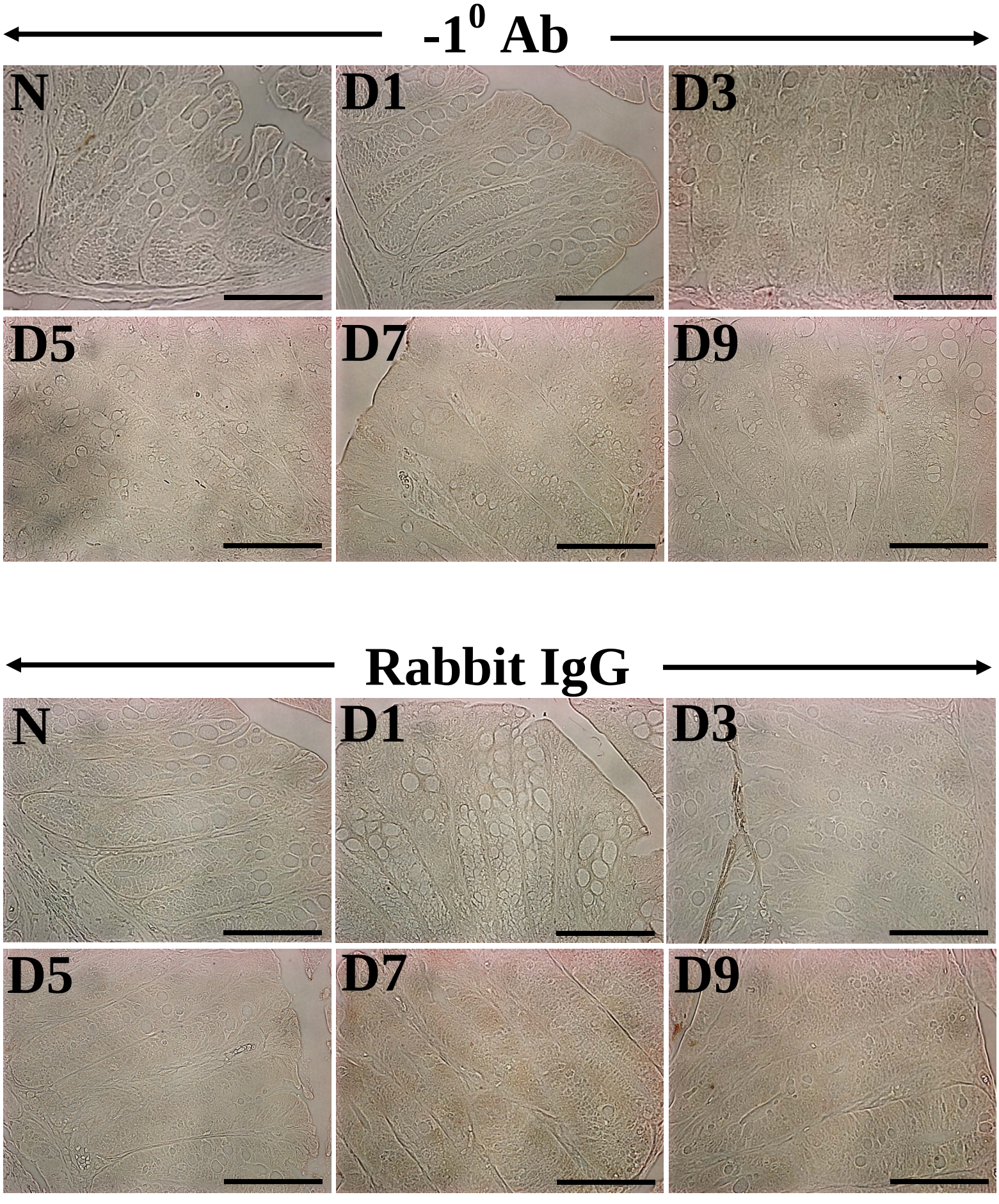

Suppl. Fig 2

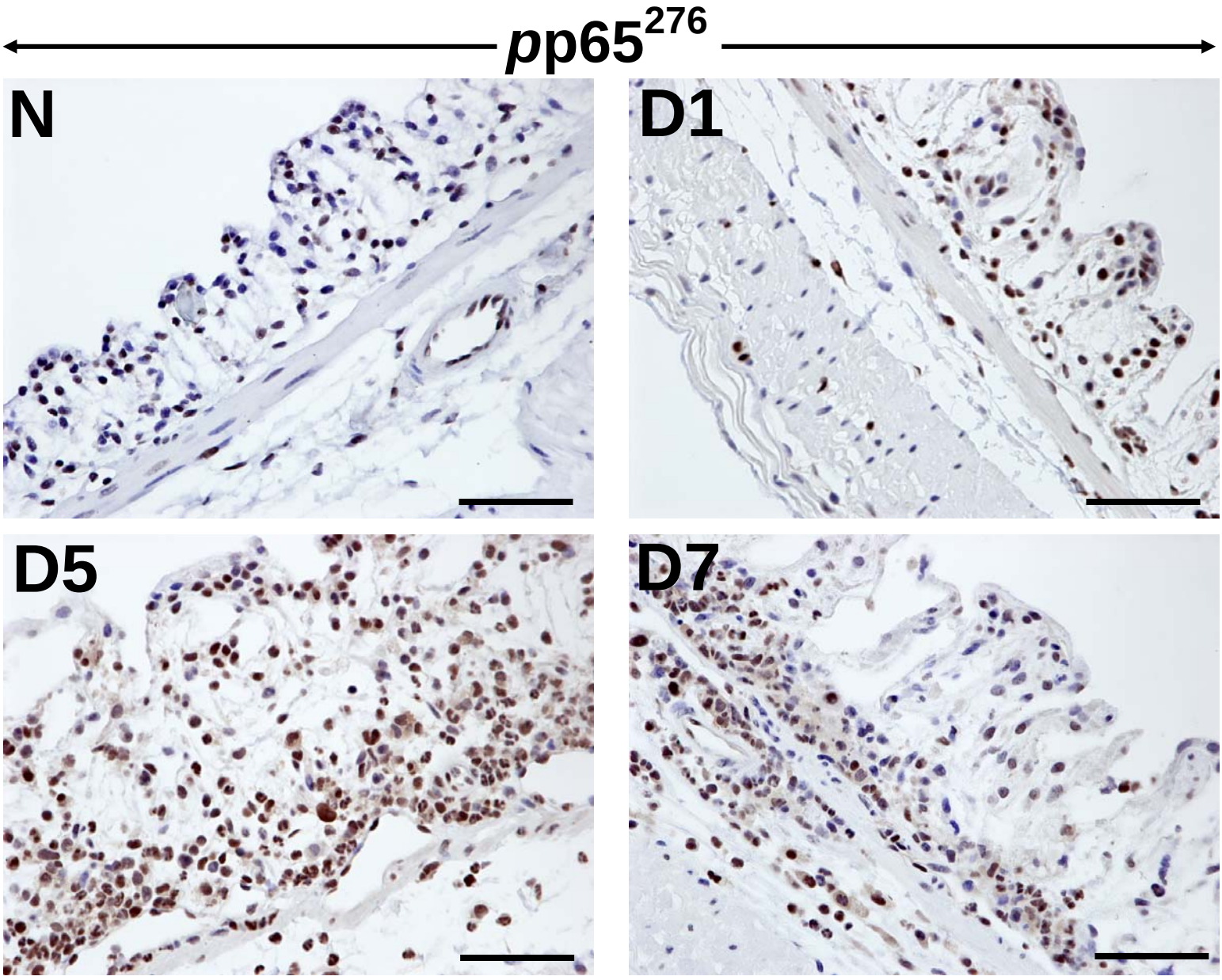

Suppl. Fig 3

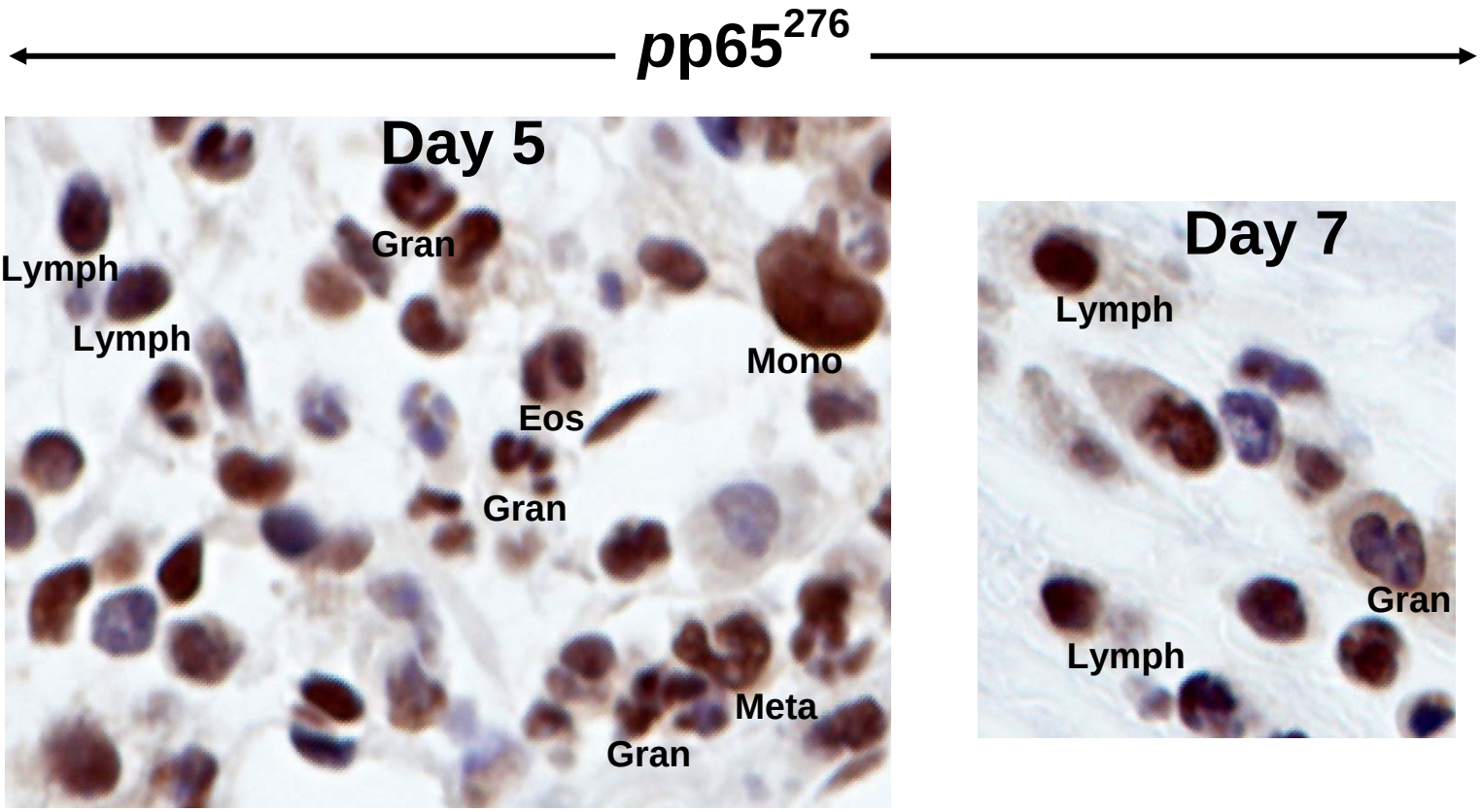
*p*p65^{276}
Day 5
Lymph
Lymph
Gran
Mono
Eos
Gran
Meta
Gran
Day 7
Lymph
Gran
Lymph

Suppl. Fig 4

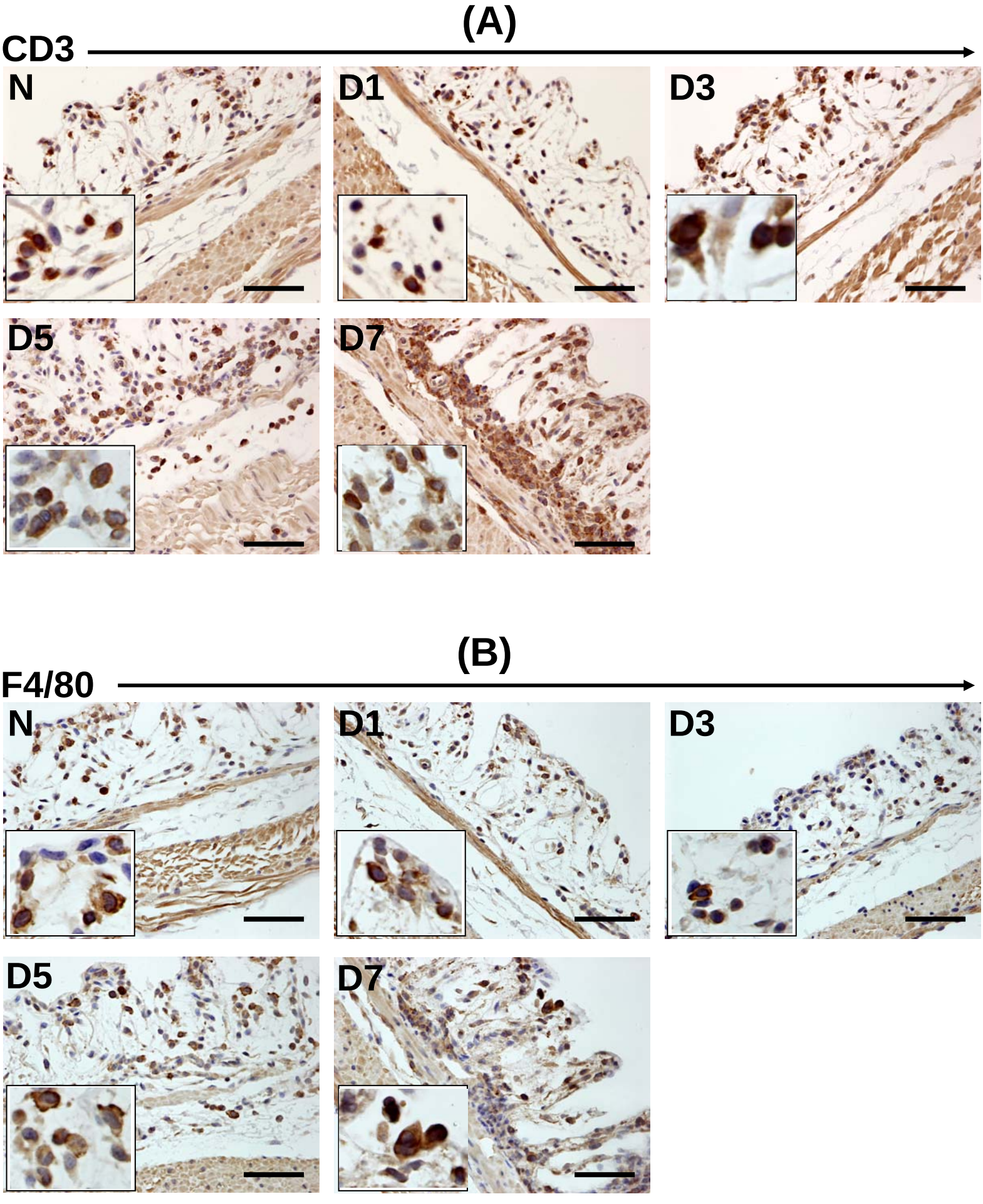

Suppl. Fig 5

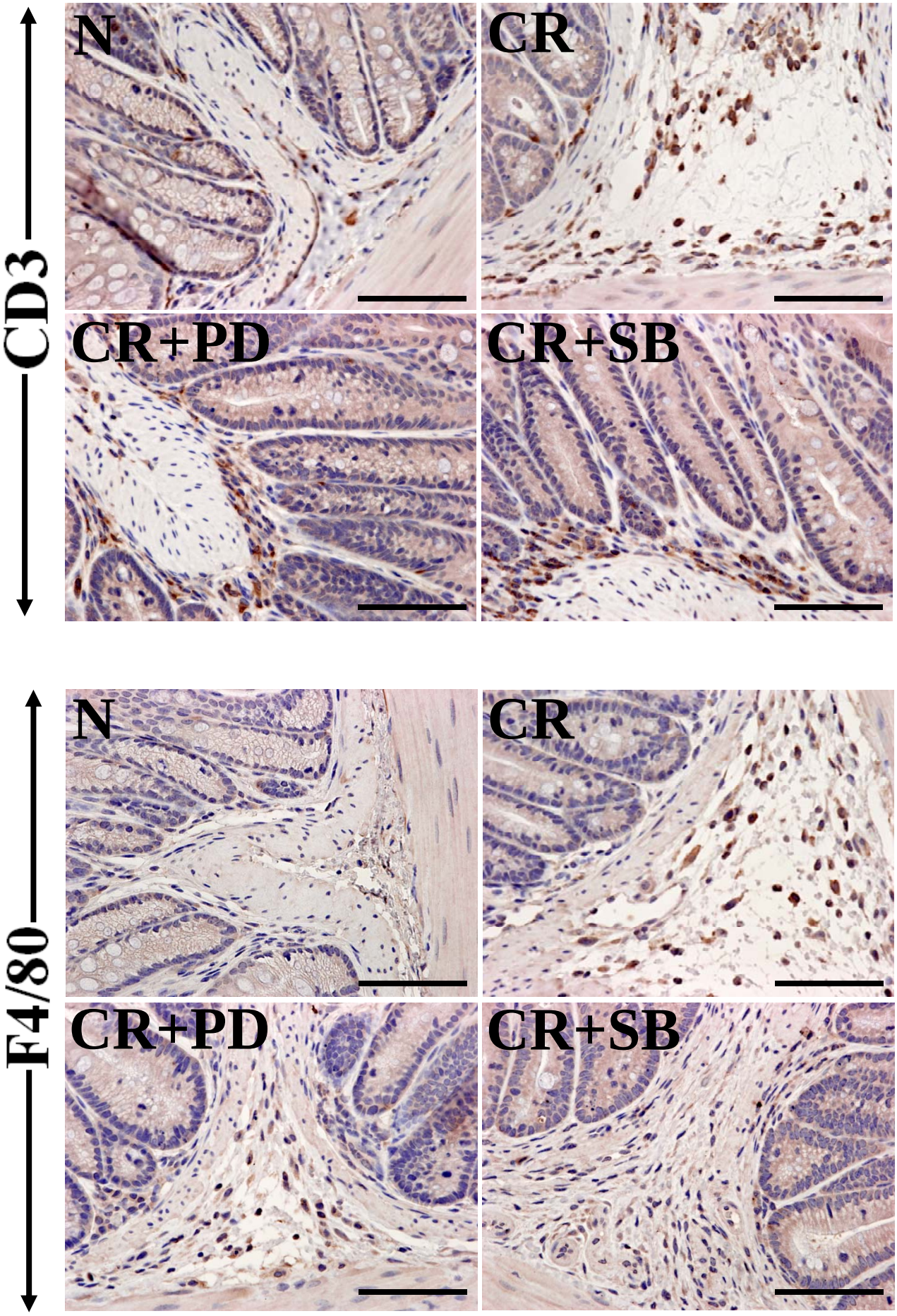

Suppl. Fig 6

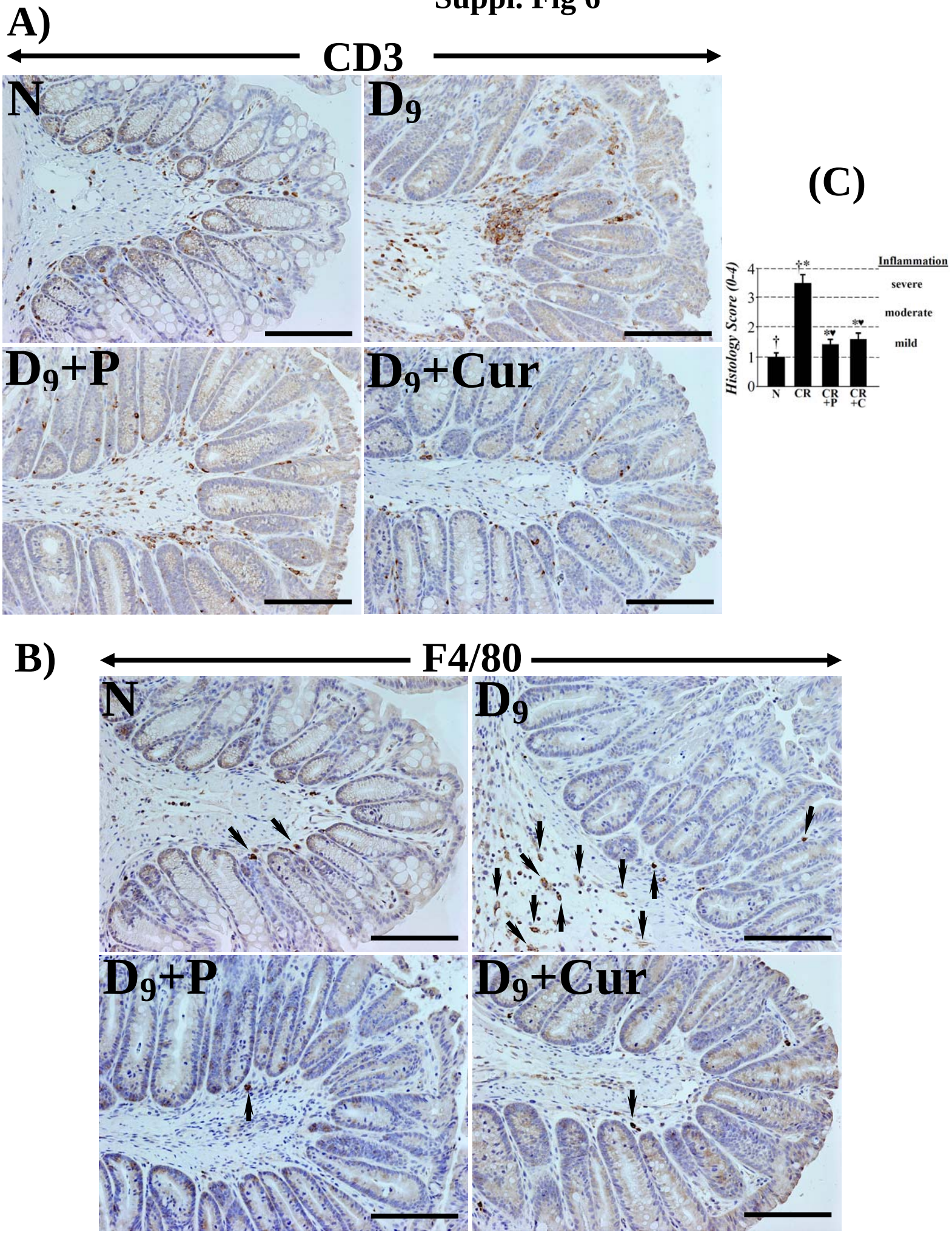
A)
CD3
N
D9
D9+P
D9+Cur
(C)
Inflammation
severe
moderate
mild
Histology Score (0-4)
0
1
2
3
4
†
†*
*♥
*♥
N
CR
CR +P
CR +C
B)
F4/80
N
D9
D9+P
D9+Cur

Suppl. Figure 7

A)

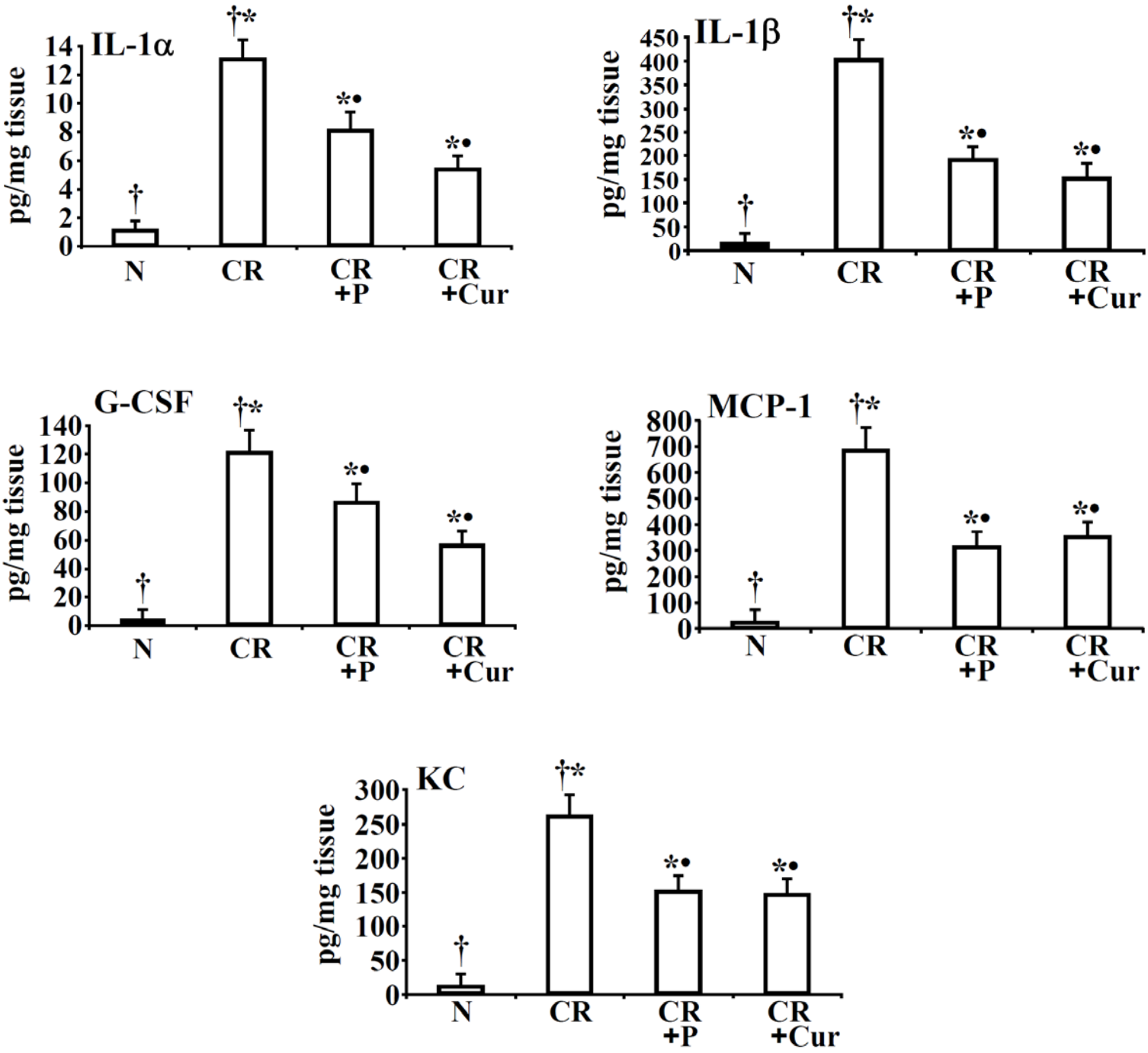

B)

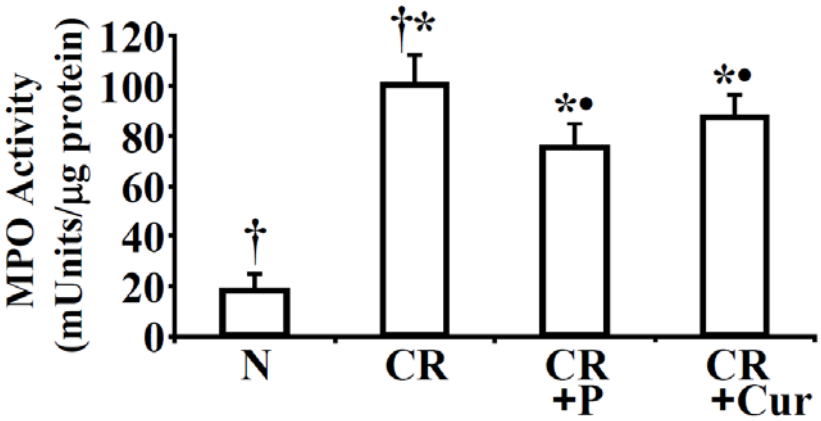

Suppl. Figure 8

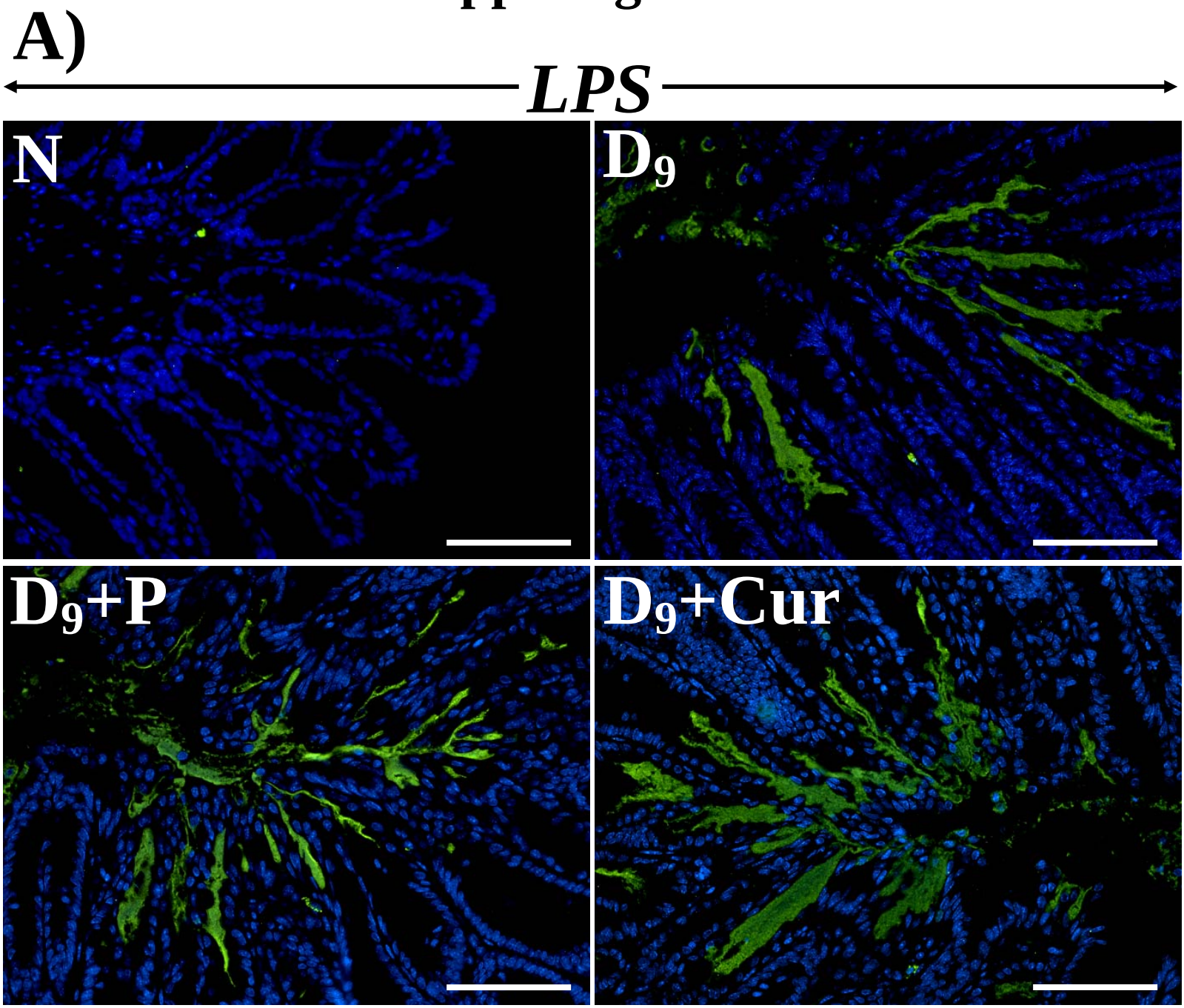

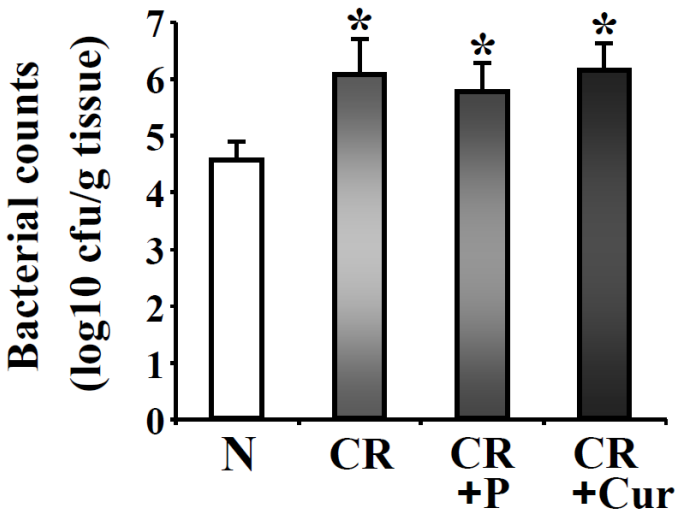

SUPPLEMENTARY FIGURE LEGENDS

Supplementary Figure 1. Immunohistochemistry either in the absence of primary antibody (upper panel) or with rabbit-IgG (lower panel) did not reveal any specific staining (Bar = 100μm; n = 3 independent experiment).

Supplementary Figure 2. Kinetics of p65 subunit phosphorylated at Ser-276 in the crypt denuded *lamina propria*. Paraffin embedded sections prepared from the crypt-denuded *lamina propria* of uninfected normal (N) and days 1-7 post-infected mice were stained with antibody for p65 phosphorylated at Ser-276 ($pp65^{276}$) and analyzed with light microscopy. Magnification = 400x; n = 3 independent experiments).

Supplementary Figure 3. Lymphocytes, monocytes and mononuclear cells stain positive for p65 subunit phosphorylated at Ser-276 ($pp65^{276}$). Crypt-denuded *lamina propria* of uninfected normal (N) and days 1-7 post-infected C3H mice were collected and processed for paraffin embedding and sections were stained with antibody for p65 phosphorylated at Ser-276 and were analyzed with light microscopy. Please note significant staining for $pp65^{276}$ in lymphocytes and monocytes/macrophages (Eos, eosinophils; Gran, granulocytes; Lymph, lymphocytes; Meta, metamyelocytes; Mono, monocytes; Magnification = 400x; n = 3 independent experiments).

Supplementary Figure 4. **Confirmation of increases in CD3+ve T-cells and F4/80+ve macrophages in the crypt-denuded lamina propria during TMCH.** Crypt-denuded *lamina propria* of uninfected normal (N) and days 1-7 post-infected C3H mice were

collected and processed for paraffin embedding and sections were stained with antibodies for CD3 (**A**) and F4/80 (**B**) to label T-cells and macrophages, respectively. Sections were analyzed with light microscopy. Insets in **A** and **B** demonstrate presence of these cells in areas denuded for crypts. Magnification = 100x, insets, 400x; n = 3 independent experiments).

Supplementary Figure 5. **Effect of p38 and p44/42 inhibitors on recruitment of T-cells and macrophages**. Representative photomicrographs of paraffin embedded sections stained with antibodies to CD3 and F4/80 to detect T-cells and macrophages, respectively. N, uninfected normal; CR, CR-infected; CR+PD or CR+SB, CR-infected and treated with specific ERK1/2 and p38 inhibitors. (Scale bar = 50μm; n = 3 independent experiments).

Supplementary Figure 6. Anti-inflammatory properties of dietary pectin and curcumin. A and B. Paraffin embedded sections prepared from the distal colons of uninfected normal (N), CR infected (day 9, D9) and CR infected (D9) + treated with 6% pectin or 4% curcumin diets were stained with antibodies for CD3 (**A**) and F4/80 (**B**) to label T-cells and macrophages, respectively. Staining was analyzed with light microscopy. Scale bar = 75μm (**A**) and 50μm (**B**); n = 3). **C**. **Measurement of histology score**. H&E stained sections from the above group of animals were subjected to measurement of inflammation and/or colitis score by an observer blinded to the treatment groups according to the morphological criteria described in Materials and Methods. †*$P<0.05$ vs. control (†); *♥$P<0.05$ vs. D9 (†*); n = 3 independent experiments.

Supplementary Figure 7. Both pectin and curcumin diets exhibit significant anti-inflammatory properties *in vivo*. A. Expression of pro-inflammatory cytokines and chemokines in the distal colonic homogenates of uninfected normal (N) and CR infected and CR infected + treated with 6% pectin or 4% curcumin mice were measured using Bio-Plex Cytokine assay Kit as described by the manufacturer. Samples were analyzed on a Bio-Rad 96 well plate reader using the Bio-Plex Array system and Bio-Plex Manager software. Each bar represents mean±SD. [†*, $p<0.05$ vs. control (†); *●, $p<0.05$ vs. CR (†*); n = 3 independent experiments]. **B. Effect of dietary intervention on myeloperoxidase (MPO) activity.** MPO activity was measured in the colonic homogenates of uninfected normal (N) and CR infected and CR infected + treated with 6% pectin or 4% curcumin mice using Fluoro MPO detection kit (Cell Tech. Inc. CA, USA) as was instructed in the manufacturer's protocol. Each bar represents mean±SD. [†*, $p<0.05$ vs. control (†); *●, $p<0.05$ vs. CR (†*); n = 3 independent experiments].

Supplementary Figure 8. **LPS staining to detect CR**. **A**. Immunofluorescence detection of LPS as a surrogate for *Citrobacter* presence in the distal colon isolated from uninfected normal (N) or CR-infected (D9) or pectin (D9+P) and curcumin (D9+Cur)-treated animals. Paraffin-embedded sections were deparaffinized, subjected to antigen retrieval and incubated overnight at 4°C with anti-LPS antibody. Following incubation with secondary antibody conjugated with fluorescein isothiocyanate (FITC), slides were analyzed by fluorescent microscopy using Axiophot 2 microscope [Carl Zeiss, Germany; Bar = 125μm; n = 5 independent experiments. Green staining represents bacterial

70 presence. **B**. **Bacterial counts**. Neither pectin nor curcumin diet had any effect on
71 bacterial counts (n = 5 independent experiments).
72